Supporting Information

Ni-loaded, Metal-Organic Framework-Graphene Composite as a Precursor for *in situ* Electrochemical Deposition of Highly Active and Durable Water Oxidation Nanocatalyst

Table of Contents

Experimental

All reagents were used as received without further purification. Solvents, and common chemicals were purchased commercially and used as received without further purification.

Nitrogen gas for sorption were purchased from Airliquide (N_2 AlphaGaz2 (99.9998%), Graphene (Alfa Aesar, catalogue 47312), Acetonitrile (analytical reagent grade 99.99%, Fisher Scientific UK), HCl (Honeywell, 37%), N,N`-Dimethylformamide (Laboratory reagent Grade, Fisher Scientific UK), Zirconium (IV) chloride (98% anhydrous, Acros Organics, USA), 2-Aminoterephthalic acid (99+%, Acros Organics, UK), Terephthalic acid (98%, Sigma Aldrich, US).

Gas sorption analysis was performed on Micromeretics **ASAP2020**. The apparent surface areas were determined from the nitrogen adsorption isotherms collected at 77 K by applying the Brunauer-Emmett-Teller (BET) model. Pore size analyses were performed using a cylinder NLDFT pore model system on oxide surface. Infra-red absorption spectra were recorded on ThermoScientific **Nicolet is-10**. Thermogravimetric analyses were conducted on Thermal Analysis-**Q50** under nitrogen atmosphere. SEM and EDX analyses were done on Nova NanoSEM 450 equipped with EDAX Octane Silicon Drift Detector (SDD). TEM images were acquired on a JEOL JEM-2100, operating at 200 KV.

XPS measurements: X-ray photoelectron spectroscopy measurements were performed using a Kratos AXIS Ultra DLD XPS system with a monochromatic Al Ka source operated at 15 keV and 150W and a hemispherical energy analyzer. The X-rays were incident at an angle of 45° with respect to the surface normal. Samples were placed in small powder pockets on the holder and analysis was performed at a pressure below $1x10^{-9}$ mbar. High resolution core level spectra were measured with pass energy of 40 eV. The XPS experiments were performed by using an electron beam, directed on the sample, for charge neutralization.

XRD measurements were conducted on PanAlytical diffractometer with Cu source ($\lambda = 1.5406$ Å) operated at 30kV and 40 mA.

Electrochemical measurements:

In a typical run, 2.25 mg of the UiO-66-NH_2-Ni@G (or the other solids) was suspended in 1 mL of isopropanol and sonicated briefly to prepare the ink of which 40 µL was drop casted on GCE of 3 mm diameter. The electrode was first polished by a P1200 sand paper, followed by 1µm polishing diamond and 0.05 µm polishing alumina, sonicated briefly in DI water and let to dry before casting. The electrochemical measurements were conducted on a biologic SP-50 potentiostat/galvanostat in a three electrodes configuration. The working electrode was a GCE casted with the prepared ink, Pt wire as a counter electrode and saturated sodium chloride calomel electrode (SSCE) as a reference electrode, the measured potential values were then converted to RHE using a standard potential of 0.236V for the SSCE vs NHE.[51] The electrolyte was aqueous KOH (1 M) either aerated or saturated with oxygen through bubbling with O_2 for 30 minutes (99.999%). Electrocatalytic response was measured using the linear sweep voltametry (LSV) technique, the cyclic voltammetry technique (CV), or controlled current chronopotentiometry technique (CP). The working electrode potential was swept at a scan rate of 10 mV/s for the LSV, while the cyclic voltammetry was measured with a scan rate of 100mV/s.

Micro-Raman Measurements

The confocal Raman-spectra were recorded using commercial system, NTEGRA spectra (NT-MDT corporation, Russia) which is equipped with a scanning stage, 3 laser excitation sources (at 488 nm, 633nm and 785 nm), a quadruple grating and an electron multiplying, Peltier cooled to -80 °C, CCD (Andor, Newton 970). In the current study, we have used 488 nm excitation. The laser beam was focused on the sample using an Olympus objective of 0.9 numerical aperture and 100× magnification thus making it easier to obtain spectra on a single graphene flake.

Synthesis of UiO-66@G

In a scintillation vial charged with magnetic stirrer, a mixture of terephthalic acid (124.6 mg, 0.75mmol) and graphene (50 mg) were mixed and sonicated in 20 ml DMF for 5 minutes to which was then added a separately prepared solution of $ZrCl_4$ (125.8 mg, 0.54 mmol) in 8 ml DMF and 2 ml HCl 37 %. The vial was capped and the mixture was stirred for 12 h at 80° C, then filtered and washed with acetonitrile (ACN), then exchanged in heated ACN at 80°C under autogenous pressure for 2h. The powder was filtered then dried in an isothermal oven at 80°C for 2 hours yielding 182.5 mg of UiO-66@G.

Synthesis of UiO-66-NH_2@G

In a scintillation vial, a mixture of 2- aminoterephthalic acid (135.86 mg, 0.75mmol) and graphene (50 mg) were mixed and sonicated in 10 ml DMF for 5 minutes to which was then added a separately prepared solution of $ZrCl_4$ (125.8 mg, 0.54 mmol) in 5 ml DMF and 1 ml HCl 37 %. The vial was capped and the mixture was stirred vigorously with the help of a stir bar for 12 hrs at 80°C in a sand bath on an isostated hotplate, then cooled to room temperature, filtered and washed with ACN, then exchanged in heated ACN at 80°C under autogenous pressure for 2 hrs. The powder was filtered then dried in an isothermal oven at 80°C for 2 hours yielding 162.5 mg of UiO-66-NH_2@G.

Synthesis of UiO-66-NH_2-Ni@G

UiO-66-NH_2@G (40 mg) and $Ni(NO_3)_2.6H_2O$ (0.58 g ,2 mmol) were mixed in 20 ml ACN and left in oven at 80°C for 1h. The solid was filtered, and then transferred into fresh ACN, kept to exchange in ACN in a sealed vial at 80°C for 1.5 h before filtering and drying at 80°C for 2h.

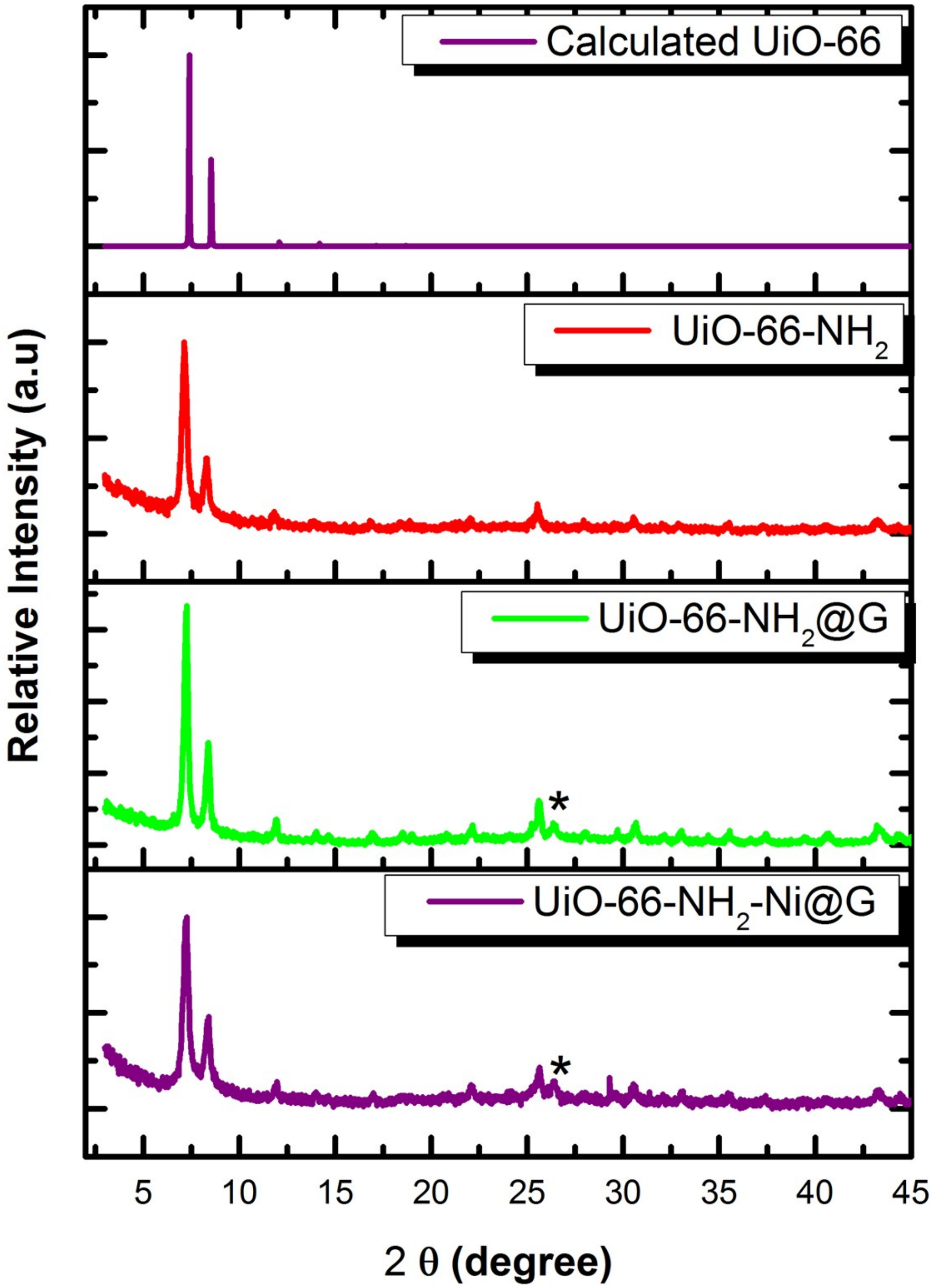

Figure S1. X-ray powder diffraction patterns for the UiO-66-NH_2, UiO-66-NH_2@G and UiO-66-NH_2-Ni@G, asterisk denotes the peak attributed to the G.

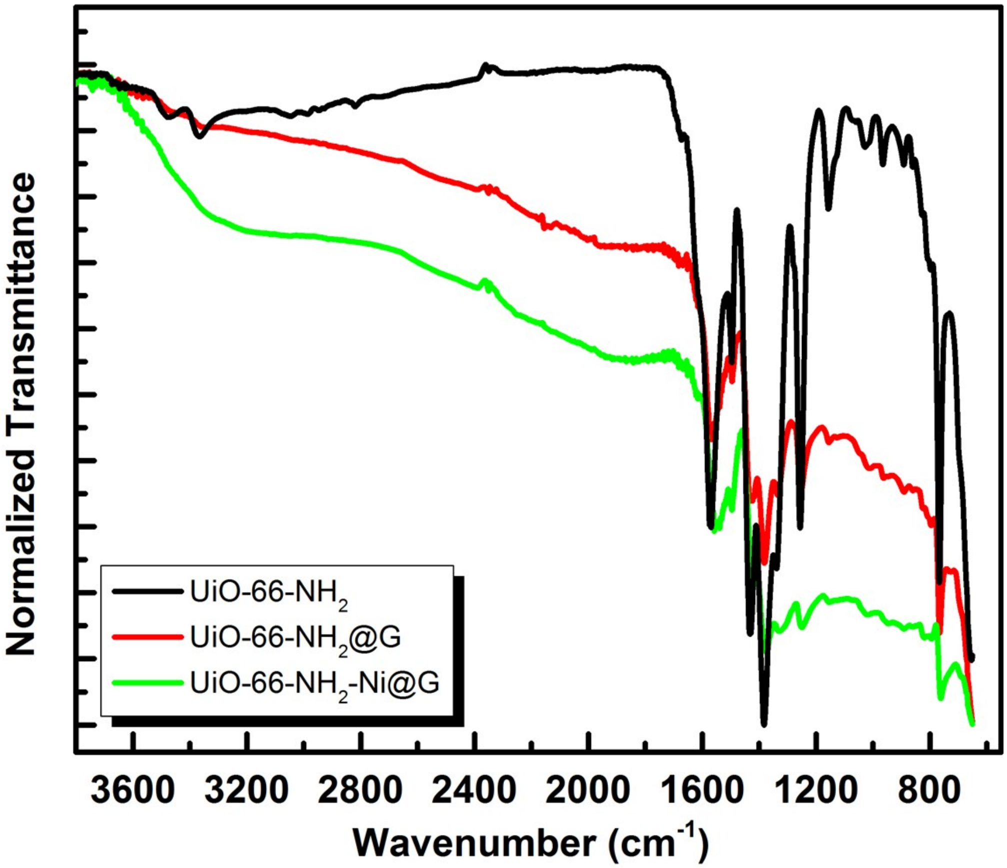

Figure S2. FTIR spectra for UiO-66-NH$_2$, the composite with G, and after Ni-metallation.

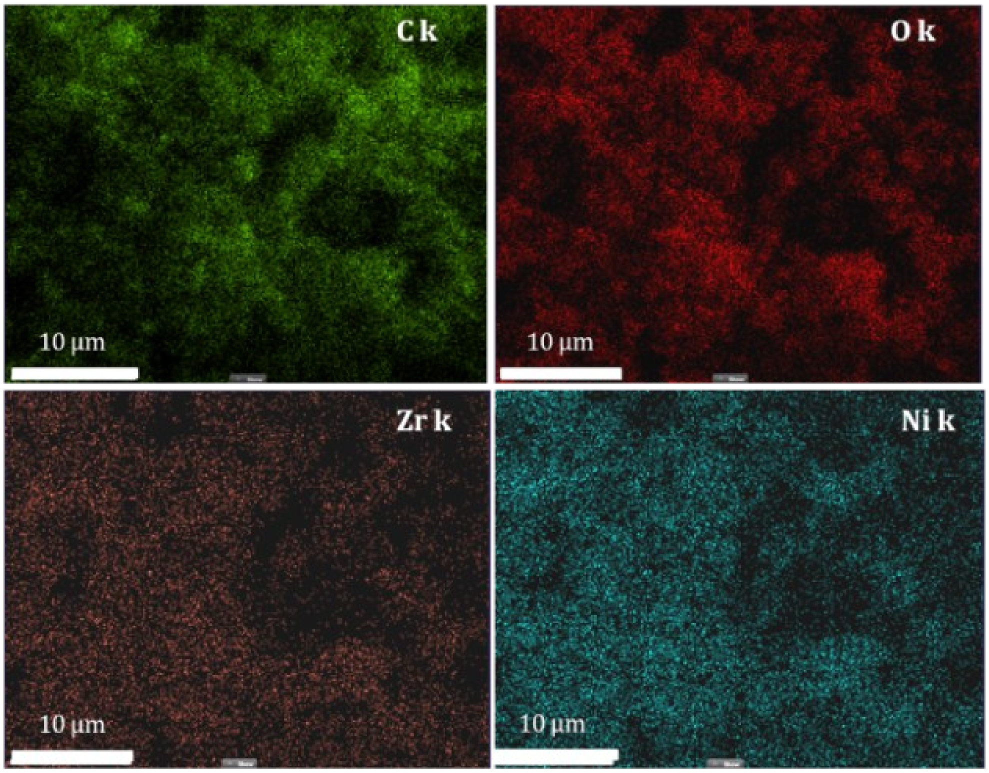

Figure S3. EDX maps for the UiO-66-NH_2-Ni@G, showing homogenous distribution of the elements (labeled images) throughout the sample.

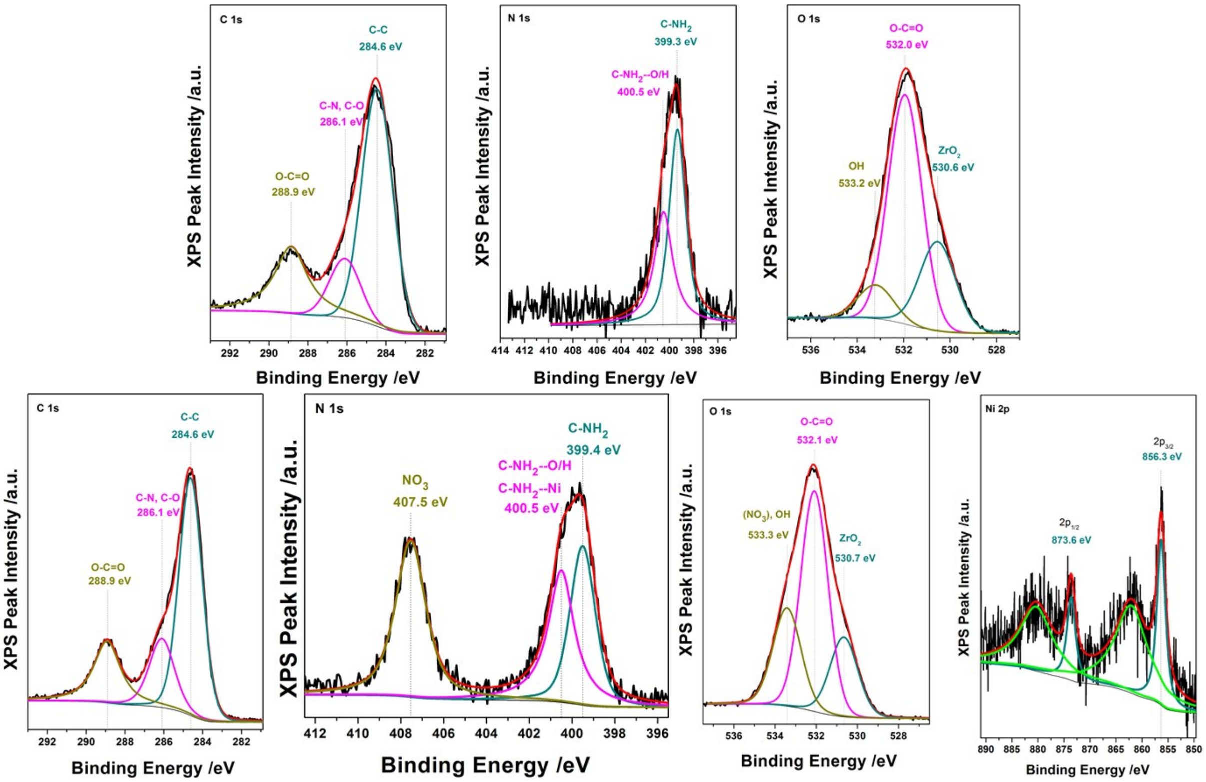

Figure S4. (top panel) XPS analysis for the UiO-66-NH$_2$@G and (bottom panel) XPS analysis for the UiO-66-NH$_2$-Ni@G showing the detailed elemental scan peaks.

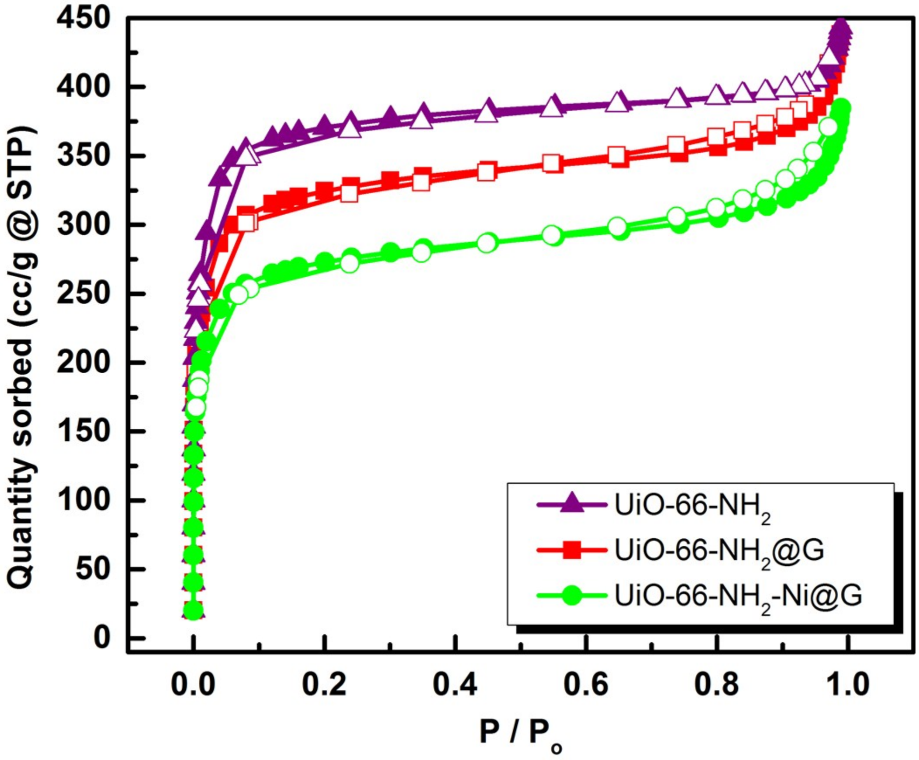

Figure S5. N_2 sorption isotherms for the UiO-66-NH_2 prepared in this study and its corresponding UiO-66-NH_2@G and after Ni metalation.

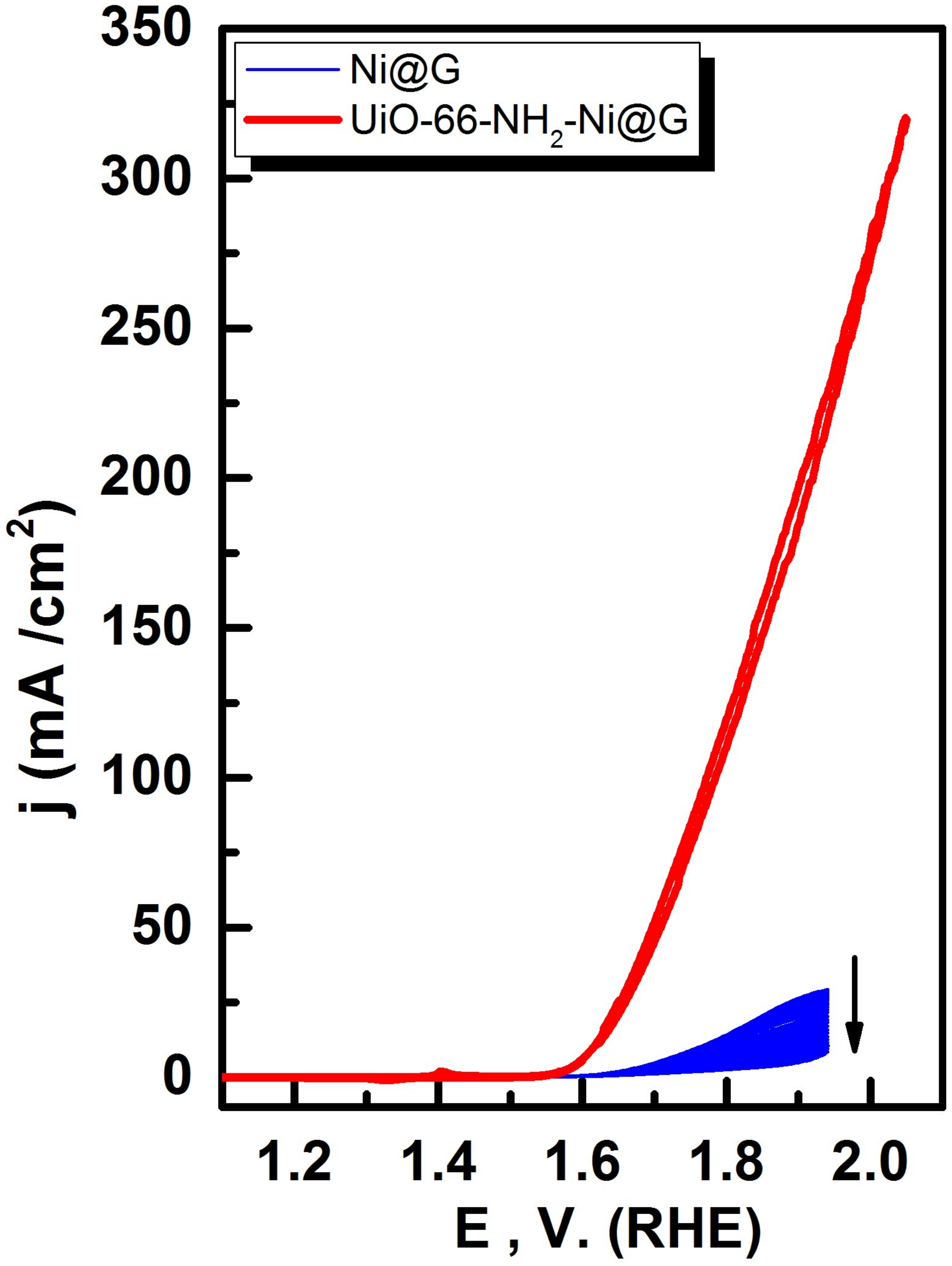

Figure S6. Cyclic voltammetry (CV) scans of the UiO-66-NH$_2$-Ni@G and Ni@G sample in 1M KOH, scan rate 100 mV/S.

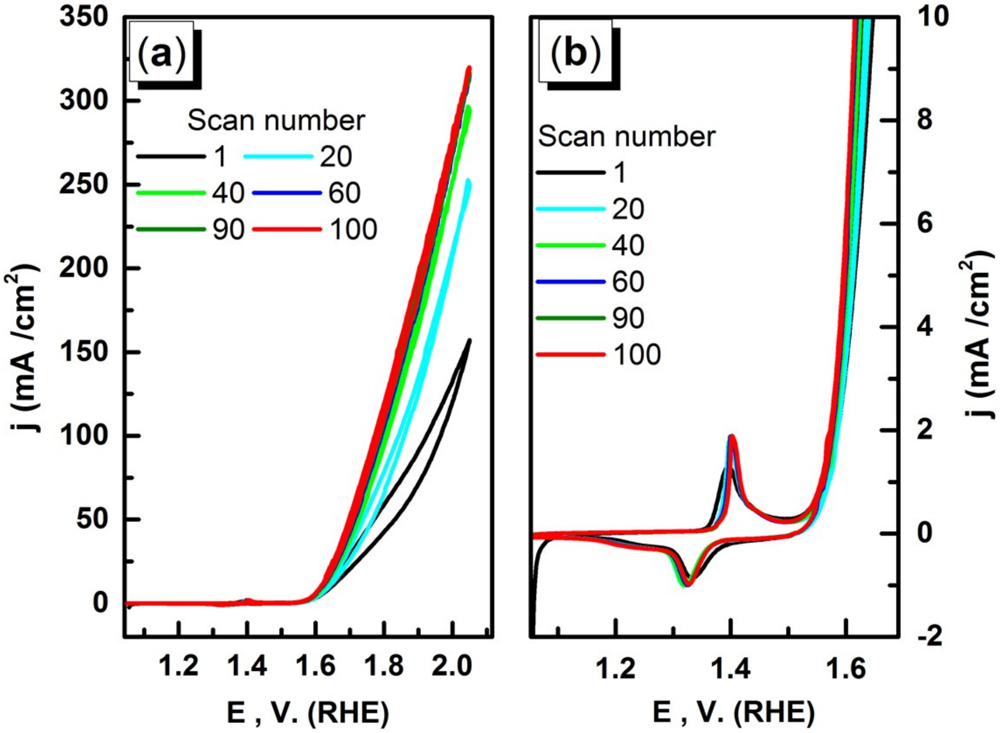

Figure S7. (a) Cyclic voltammetry (CV) scans of the UiO-66-NH_2-Ni@G and (b) magnified part of the plot showing the peaks for Ni(II/III) redox pair, in 1M KOH, scan rate 100 mV/S.

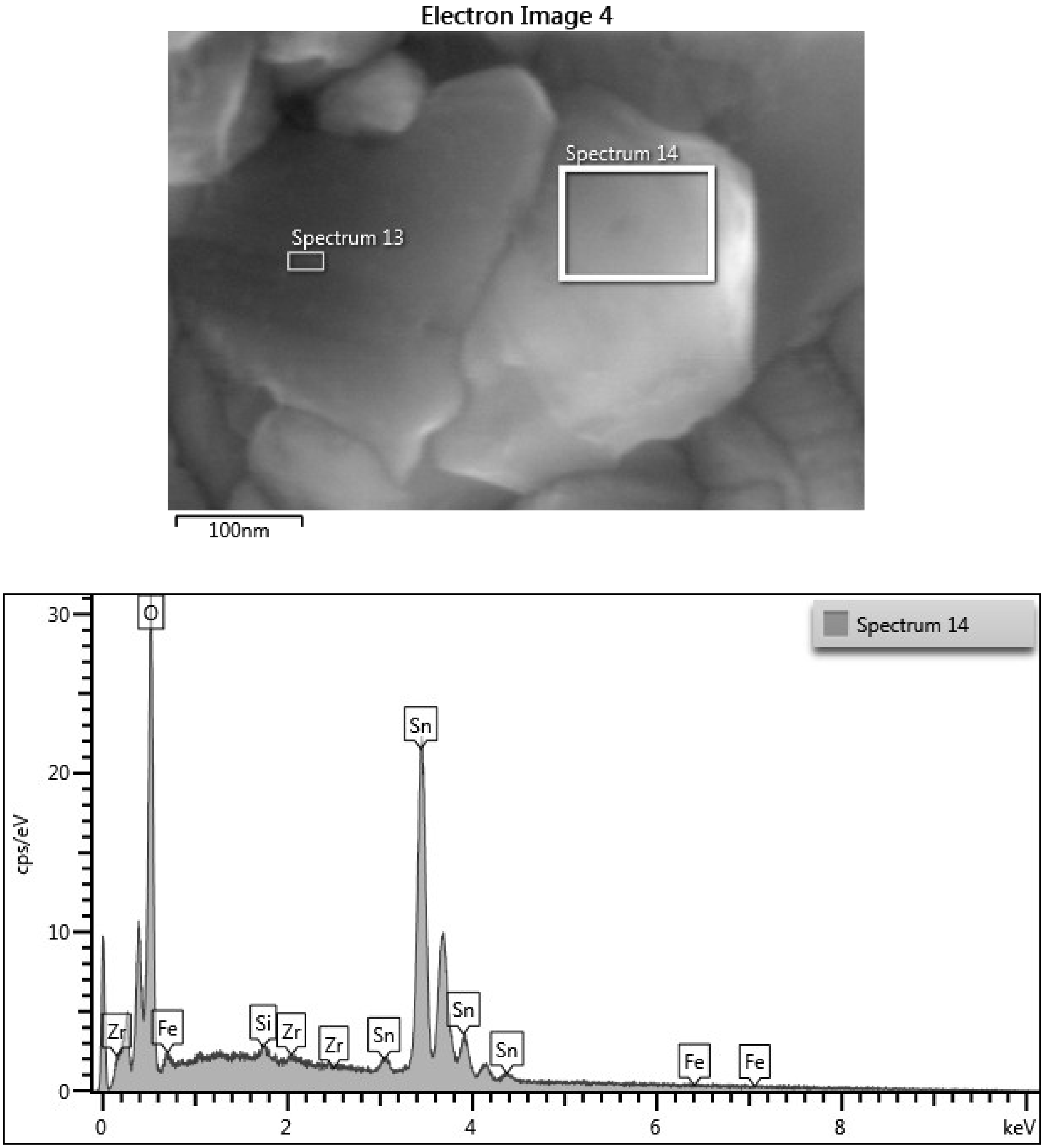

Figure S8. (top) SEM image of the FTO electrode surface and (below) the corresponding EDX elemental analysis.

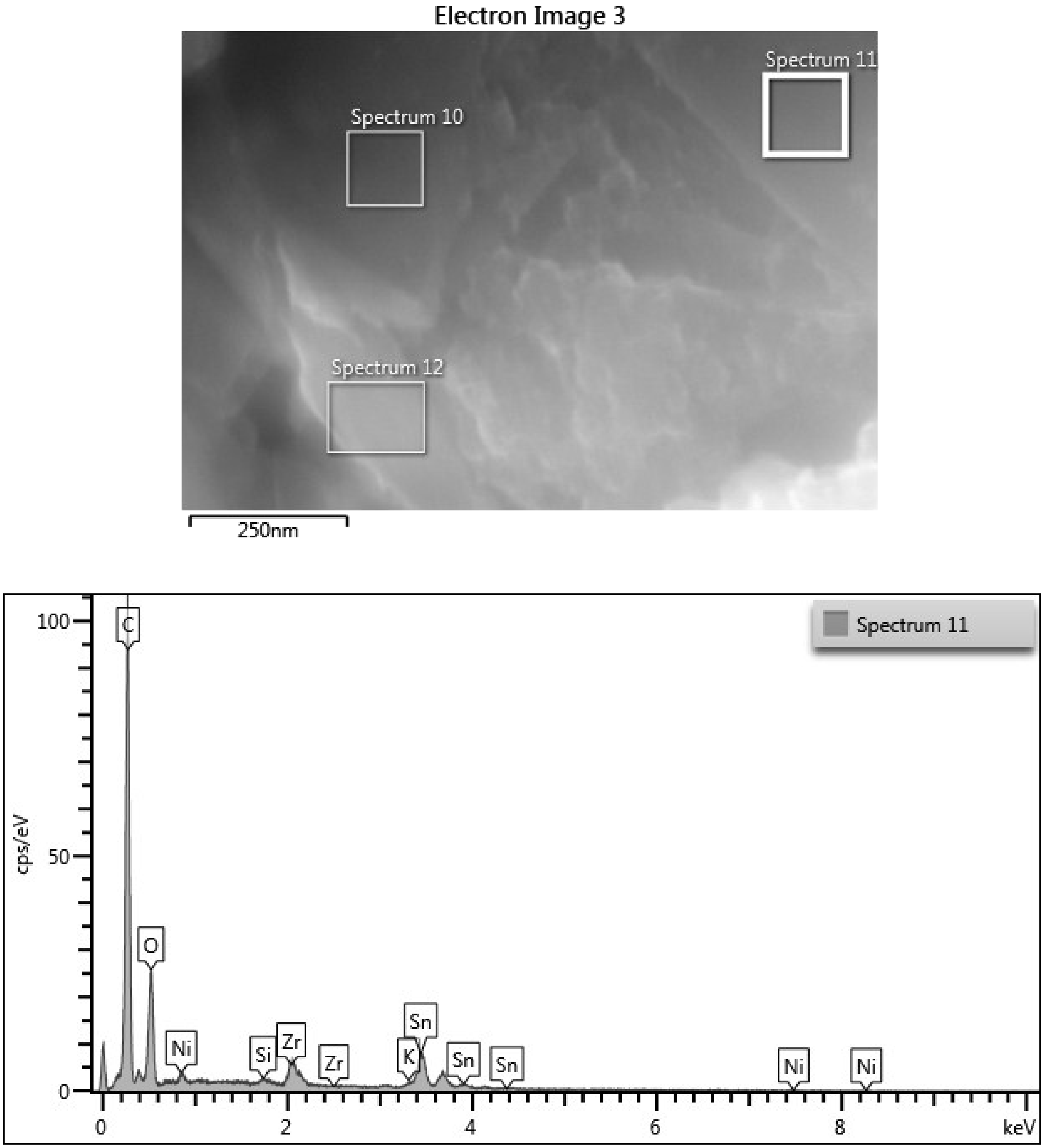

Figure S9. (top) SEM image of the $Ni(OH)_2$-ZrO_2@G on the FTO electrode surface after the electrochemical measurements, and (below) the corresponding EDX elemental analysis.

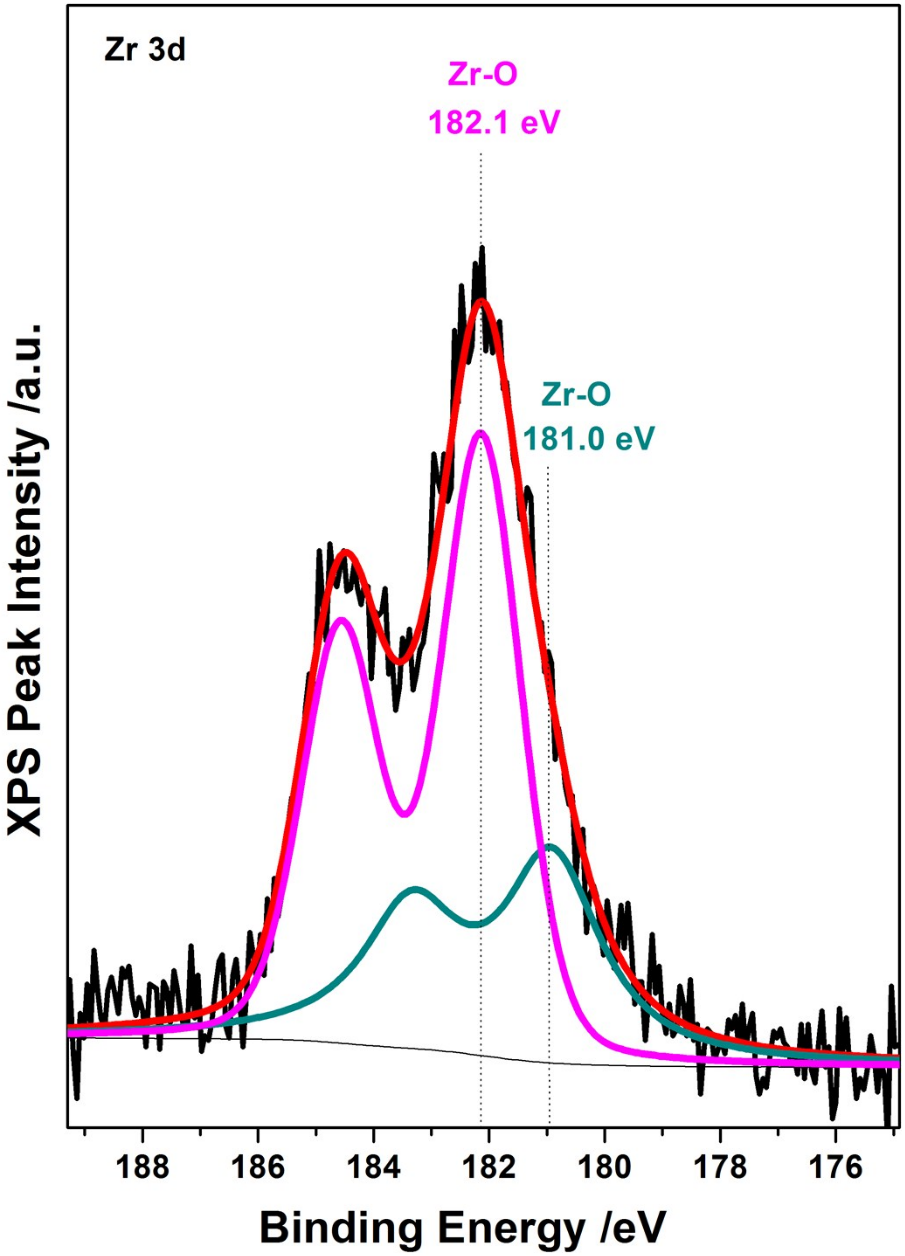

Figure S10. XPS detailed spectrum of Zr after the electrolysis in 1M KOH.

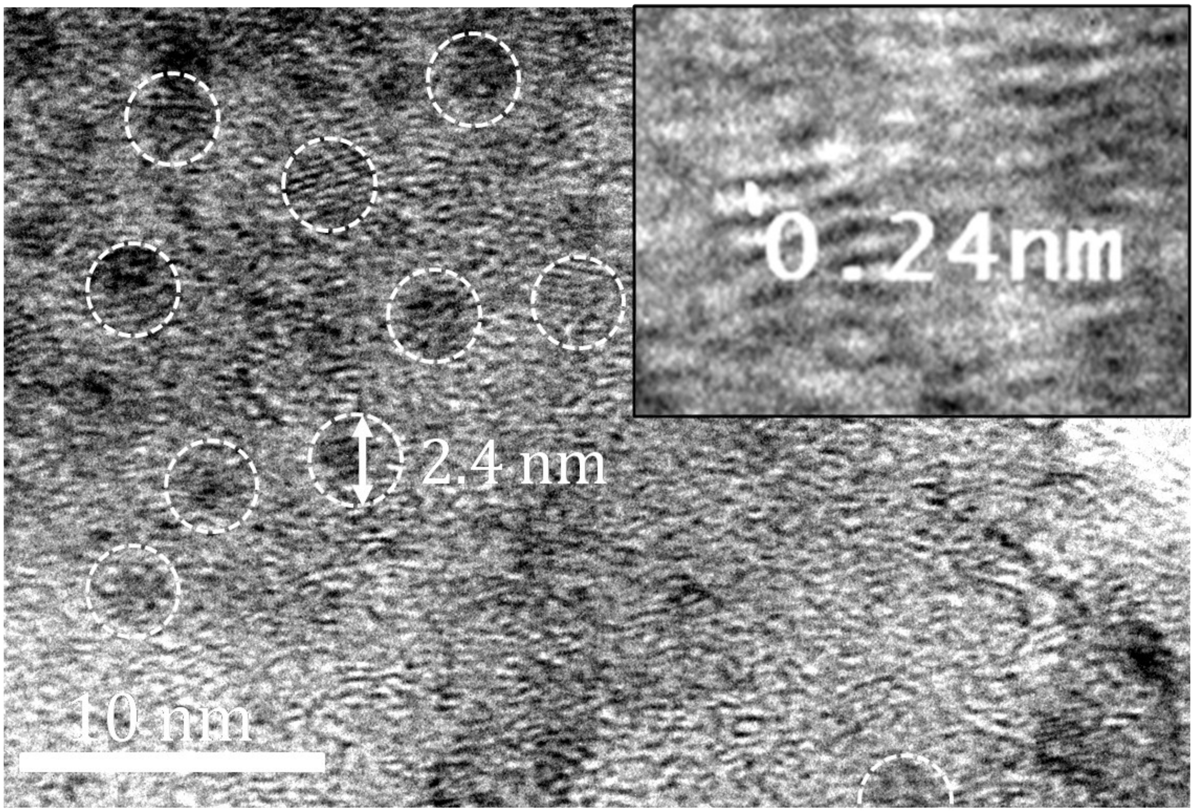

Figure S11. TEM image of the catalyst after electrolysis, showing $Ni(OH)_2$ nanoparticles on G sheets, insert showing interplanar distance.

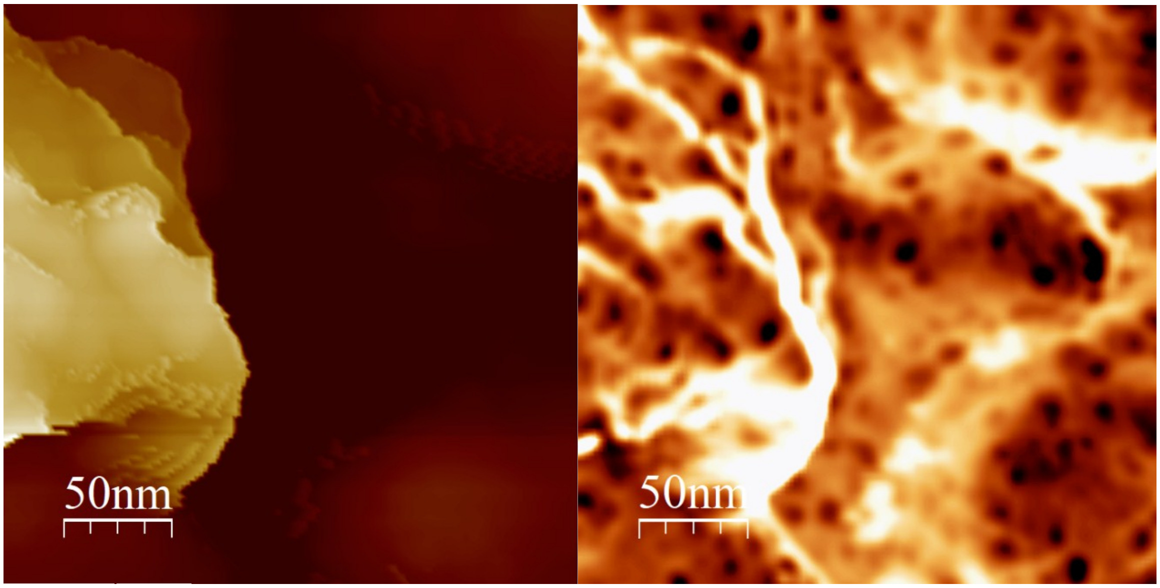

Figure S12. AFM topographic (left) and the corresponding phase (right) images of the catalysts after electrolysis. The black spots are due to clusters of $Ni(OH)_2$ nanoparticles on G sheets.